Title
CONFIGURATION INTERACTION EFFECTS IN THE ATOMIC PHOTO-ELECTRON SPECTRA OF Ba, Sm, Eu, AND Yb

Author
Lee, S.-T.

Publication Date
1976-10-01

Submitted to Journal of Chemical Physics

LBL-5703
Preprint

CONFIGURATION INTERACTION EFFECTS IN THE ATOMIC PHOTOELECTRON SPECTRA OF Ba, Sm, Eu, AND Yb

S.-T. Lee, S. Süzer, E. Matthias,
R. A. Rosenberg, and D. A. Shirley

October 1976

Prepared for the U. S. Energy Research and Development Administration under Contract W-7405-ENG-48

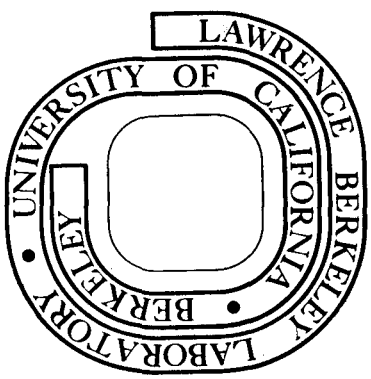

DISCLAIMER

CONFIGURATION INTERACTION EFFECTS IN THE ATOMIC PHOTOELECTRON SPECTRA OF Ba, Sm, Eu, and Yb*

S.-T. Lee, Ş. Süzer, E. Matthias,†
R. A. Rosenberg, and D. A. Shirley

Materials and Molecular Research Division
Lawrence Berkeley Laboratory
and
Department of Chemistry
University of California
Berkeley, California 94720

ABSTRACT

High temperature photoelectron spectra of Ba, Sm, Eu, and Yb were studied using both HeI and NeI resonance lines. In addition to strong lines corresponding to transitions from the primary configurations, correlation satellites were observed in every spectrum. By comparing the spectra excited at different photon energies, the satellite lines found in all NeI spectra and the HeI spectrum of Yb were attributed to admixtures of the configurations $5d^2$, $6p^2$, etc., into the ground state. Autoionization is believed to occur at the energies of the HeIα, HeIβ and NeI satellite lines for Ba, at the HeIα energy for Sm, and at the HeIα and HeIβ energies for Eu. Autoionization was detected by noting the dramatic increase in satellite intensities and, in some instances, the large deviation of the observed intensity ratios within multiplets from the statistical values. Photoelectron spectroscopy has been demonstrated to have great potential in providing detailed information about electron correlation in both initial and final states.

---

*This work was done with support from the U. S. Energy Research and Development Administration.

†Permanent address: Freie Universität Berlin, West Berlin, Germany.

I. INTRODUCTION

The origin of satellite lines due to electron correlation in photoelectron spectra has recently been discussed[1,2] using the model of configuration interaction (CI). Photoionization causes a transition from an initial state of an N-electron system to a final state composed of an (N-1)-electron ion and the free electron. Within the context of a particular basis set, the intensities of the correlation satellites can derive contributions from configuration interaction in the initial (ISCI) and/or final state. For pedagogical purposes, final-state CI can further be classified as final ionic CI (FISCI),[1,2] continuum state CI (CSCI),[2] and autoionization.[3] Among these four mechanisms leading to satellites, autoionization is readily distinguishable because of its resonant nature. The distinction among the other three is not so straightforward; indeed this distinction is unique only within the context of a particular basic set. In the case of the Ne 1s satellites, elaborate CI calculations were necessary in order to establish the major contributions from ISCI and FISCI, and to bring the calculated intensities into agreement with experiment.[4] However, in certain atomic cases, ISCI can be regarded as the sole dominant contributor to the satellites[5] simply on the grounds of symmetry and near-degeneracy of states. Therefore, ISCI was found predominantly responsible for the satellites in the photoelectron spectra of Pb,[6] Bi,[7] and Group-IIA and -IIB elements.[5,8,9] Particularly in these latter cases, satellite structure can provide unique information about the nature and extent of electron correlation effects in the ground states of atoms.[5]

Continuing our work with metal vapors, we have made a similar study on some rare-earth metals. Because of the similar valence-electron configurations of the rare-earths and the alkaline earth metals, we expect to find ISCI satellites in the photoelectron spectra of the former as well. Furthermore, it is interesting to see what effects the incompletely-filled 4f-shell will have on the satellites.

Recent studies, both experimental[10-12] and theoretical,[13,14] have suggested that resonant autoionization might be responsible for the remarkably high intensities of satellites and the large ratio of double to single ionization in the photoelectron spectra of Ba excited by HeIα(21.22eV) line. The resonant absorption at HeIα energy is further demonstrated by comparison to the NeI spectrum of Ba[5], and by the UV absorption spectrum of Ba in the 800-500 Å region.[15,16] The Rydberg-like state reached by the HeIα line must involve one of the $5p^6$ electrons, on energy grounds, possibly a state like $[5p^5\ 6s^2(nd \text{ or } ns)]_{J=1}$. Proceeding from Ba to the lanthanides, because of the rather effective screening of the additional nuclear charge by the accompanying additional 4f-electrons, we expected the threshold of 5p ionization to increase only gradually with the filling of the 4f shell. Therefore, it was anticipated that the HeIα line would be close to the 5p threshold, and that resonant absorption might occur at HeI resonance energies for some lighter lanthanides. In light of the above discussion, it might thus be possible to extend the observation and study of autoionization with laboratory source from barium into the lanthanides.

In this paper, we report the observation of satellites in the UV photoelectron spectra of Ba, Sm, Eu, and Yb. By analysis of the spectra provided by the various He and Ne resonance lines, satellites due to ISCI and autoionization have been differentiated.

Experimental information is given in Section II, and results and assignments are given in Section III. In Section IV these results are discussed in terms of autoionization and other mechanisms. Conclusions are drawn in Section V.

II. EXPERIMENTAL

The experimental procedure is identical to that reported earlier.[5,6] Briefly, the spectra were taken with a modified Perkin-Elmer PS-18 photoelectron spectrometer. The samples were loaded in air in a stainless steel container which rested inside the ionization chamber that was heated by a tantalum oven. Because of continuous deposit and oxidation of the metals on critical surfaces, the resolution of the electron analyzer could vary considerably during a run, which lasted between one and ten hours with a single sample load. The resolution also changed with the electron energy, and ranged between 60 and 150 meV for 9 eV electrons as monitored by the Xe $^2P_{3/2}$ line. Energy calibration was done by measuring Xe and N_2 photoelectron lines together with the sample, and also by using the documented first ionization potentials of the metals. All samples were obtained in purities of 99% or higher from commercial sources.

Intensities of lines were taken as the peak areas divided by their kinetic energies (thereby correcting for the theoretical transmission function of the analyzer). No correction was made for the

dependence of transmission upon charging effects and inelastic scattering; nor has the effect of photoelectron angular distribution been taken into account. Therefore the reported intensities bear large uncertainties and are only included for qualitative discussion. However, the relative intensities of lines that lie nearby in energy in the same spectrum are expected to be quite reliable. In the case of Ba, HeII and NeII lines were necessary to ionize the 5p electrons. These more energetic lines were produced using a hollow cathode lamp.[17]

The temperatures at which the spectra were recorded are: Ba/HeI (620°C), Ba/NeI (700°C), Sm/HeI (640°C), Sm/NeI (730°C), Eu/HeI (740°C), Eu/NeI (740°C), Yb/HeI (650°C), and Yb/NeI (600°C). The thermocouple which monitored the temperature was in contact with the colder part of the oven;[6] hence the actual sample temperatures may be up to 30°C higher than those given.

III. RESULTS AND ASSIGNMENTS

The spectra of Ba, Sm, Eu, and Yb are displayed respectively in Figs. 1-4, with the prominent lines labelled. The peaks marked S are assigned to photoemission induced by HeI or NeI satellite lines and those denoted I are inelastic loss peaks of the intense lines involving the $6s \rightarrow 6p$, $\Delta S = 0$ and $\Delta L = 1$ transitions. The results and derived parameters are collected in Tables 1-4, and Table 5 gives the energies and relative intensities of the HeI and NeI lines produced in our lamp. Except as noted, the photoelectron lines were identified by comparison with the ionization potentials from optical work.[18] The spectra of the four elements are discussed separately below.

A. $Ba(6s^2;{}^1S)$

In agreement with previous workers,[11,12] the HeIα spectrum of Ba (Fig. 1a) shows a large number of excited ionic states with remarkably high intensities. With better statistics, we have been able to positively detect and identify several new lines in the energy range 13-15 eV (Table 1). All lines below 14.2 eV are associated with the Ba^+ states of $5p^6n\ell$ configurations, with ℓ representing s, p, d, f, and g orbitals and the number n going as high as 10 for s and p orbitals. The lines numbered 4-10 may be assigned similarly to the higher Rydberg states ($5p^6n\ell$) of Ba^+ leading to the threshold of Ba^{++} at 15.215 eV,[18] as proposed previously,[11] but alternative assignments may be possible, as discussed later (Section IVD). The nature of the three intense lines lying above the threshold of Ba^{++} has been unequivocally established by Hotop and Mahr[12] as arising from two-step double ionization, forming Ba^{++}. The peak at 3.34 eV and the doublet at 4.0 eV are the 6s and 5d states of Ba^+ reached by the HeIβ line.

The NeI spectrum above 3 eV has been reported earlier,[5] but is included here for comparison and to show the ionization due to other, weaker NeI lines. Except for the 6s Ba^+ ground state, only 5d, 6p, 7s, 6d, and 4f states are positively detected and are of much lower intensity relative to the 6s line in HeIα spectrum. The lines in the 1-3 eV range (Fig. 1b) cannot be assigned to any states of Ba^+ resulting from excitation by the NeI doublet. These lines have been reproduced in two independent runs and the possibility of their arising from impurities having 2-3 eV binding energies is very small. We attribute these peaks to 5d and 6s Ba^+ states excited by the weak NeI satellite lines between

19.69 and 21.11 eV (Table 5). These peaks are broadened and coalesced by the instrumental resolution.

Ionization of Ba by HeII (40.8 eV) and NeII (26.9 eV) has also been studied in an attempt to determine the $(5p)^{-1}$ threshold. In both spectra, a peak corresponding to a binding energy of 22.7 eV was detected. This peak is assigned to the ionic state $(5p^5 6s^2; {}^2P_{3/2})$ by comparison to a $(5p)^{-1}$ hole state relativistic Hartree-Fock calculation using the Desclaux program,[19] which gave $(5p_{3/2})^{-1}$ hole states at 22.15 and 24.28 eV respectively. The assignment is further corroborated with the results obtained from the Auger spectrum of Ba,[20] which gave the $(5p_{3/2})$ and $(5p_{1/2})$ binding energies at 22.7 and 24.8 eV. The $(5p^5 6s^2;\ {}^2P_{1/2})$ state was, however, not detected in the HeII spectrum because it is overlapped by the $Ba^+ 6s$/HeI line or in NeII spectrum presumably due to poor electron collection efficiency.

B. $Sm(4f^6 6s^2; {}^7F_o)$

Both HeI and NeI spectra of Sm (Fig. 2) shows four bands centered at 5.8, 8.9, 9.6 and 11.9 eV. The band at 5.8 eV is associated with the removal of a 6s electron giving the ${}^8F$ and ${}^6F$ manifolds of the $[4f^6({}^7F)6s]$ configuration. However this band shows quite different structure in the two spectra. In the NeI spectrum it consists of two sharp peaks at 5.64 and 5.80 eV, while in HeI it is made of a sharp peak at 5.64 eV and a band with 0.34 eV FWHM at 5.80 eV. The bands at 8.9, 9.6, and 11.9 eV are similar in both spectra and have, respectively, FWHM values of 0.6, 0.4, and 1.2 eV. They are associated, in the same order, with the ${}^6H$, ${}^6F$, and ${}^6P$ terms of the Sm^+ $(4f^6 6s^2)$ configuration (see below). The HeI spectrum shows additional electron

intensity between 6.5 and 8.0 eV, and possibly also on the low energy shoulder of the ^6H manifold, although the NeI spectrum also shows an indication of weaker signals around 7 eV. The five peaks in the range 6.5 - 8.0 eV in the HeI spectrum correspond to Sm^+ states from the $4f^6(^7F)5d$ configuration, and their widths suggest more than one state within each peak. The intensity around 8.4 eV may be assigned to states from the $4f^6(^7F)6p$ configuration. The broad band centered at 10.5 eV, present only in the NeI spectrum, intensified with increasing temperature and seemed to grow relative to the other peaks with elapsed running time. It is difficult to assign the band to inelastic losses in view of its high energy, and we tentatively attribute it to impurities.

The ground state of $Sm(4f^66s^2)$ is $^7F_0$, but at ca. 1000 ^0K, the $^7F_{J=1,2,3,4,5,6}$ components are also populated. Using the energy splittings of the J components,[18b] we estimated their population ratio in the order of increasing J values to be 1.0 : 2.0 : 1.5 : 0.84 : 0.36 : 0.11 : 0.04. Since all J components of ^7F are populated, removal of a 6s electron from $[4f^6(^7F)6s^2]$ should give ^8F and ^6F terms with all the possible J values, although the lower J's are favored due to larger population of low J's in the initial state. Despite the many possible final states, it can be readily shown that both the ^8F and ^6F manifolds have energy spreads of only ca. 0.10 eV and are separated by at least 0.14 eV. This result is in good agreement with the first doublet in the NeI spectrum. Removal of a 4f-electron from the $4f^6(^7F)6s^2$ state results in ^6H, ^6F, and ^6P states and their intensity, ratios can be related to the squares of the fractional parentage coefficients,[21]

which are respectively 0.52, 0.33, and 0.14.[22] The energies of these terms for the free atoms has not yet been determined. Brewer[23] estimated the $^6H_{5/2}$ state of Sm^+ to be at (8.61 ± 0.25) eV. This value compares well with the threshold 8.6 eV of the band at 8.9 eV, and thus supports our assignment of this band to ^6H. The positions of the ^6F and ^6P states relative to ^6H can be estimated from the known intervals in the $Sm^{+3}(4f^5)$ ion. The justification for such estimation is that the 6s electrons have little screening effect on the 4f electrons. For Sm^{+3}, the weighted centers of the ^6H, ^6F, and ^6P terms are respectively 0.36, 1.11, and 3.11 eV above the $^6H_{5/2}$ state.[24] In Fig. 2a, these estimated positions are indicated by bars with lengths proportional to the squares of respective fractional parentage coefficients of the ion states. There is very good agreement between the observed and predicted energies and fair agreement in relative intensities. The J components of ^6H, ^6F, and ^6P terms for Sm^{+3} spread over respectively 0.6, 0.4 and 0.3 eV. While the widths of ^6H and ^6F terms are in perfect agreement with those observed for the bands at 8.9 and 9.6 eV, the width of ^6P is much smaller than that (1.2 eV) of the band at 11.9 eV. If spin-orbit coupling is strong enough in the $4f^56s^2$ configuration, then other states besides the three sextets can be accessible as a result of the mixing in the final ionic states. These additional states would fall close to the ^6p states[22] and contribute to the observed band width. In light of the above considerations, our assignment of $Sm^+(4f^56s^2)$ states should be reliable, and the photoelectron spectra represent the first determination of the positions of the ^6H, ^6F, and ^6P states in Sm^+.

C. Eu($4f^7 6s^2$: ^8S)

The peaks between 5.6 and 9.1 eV, except for the inelastic loss peaks at 8.34 and 8.56 eV, in both the HeIα and NeI spectra, shown in Fig. 3, are associated with the Eu^+ states of the configurations [$4f^7(^8S)6s$], [$4f^7(^8S)5d$], and [$4f^7(^8S)6p$]. These seven peaks correspond, as indicated in the spectrum, respectively to the states ^9S, ^7S, $^9D_{6,5,4,3,2}$, $^7D_{1,2,3,4,5}$, $^9P_{4,3}$, $^9P_5$, and $^7P_{2,3,4}$ by comparison to optical data.[18c] The electron distribution around 10.2 eV is assigned to the $^7F_{0,1,2,3,4,5,6}$ states of $Eu^+[4f^5(^7F)6s^2]$, whose positions have not been determined before. This assignment is substantiated by the close agreement between our energy for the $^7F_0$ state and that calculated by Brewer[23], i.e., (9.99 ± 0.05) and (9.76 ± 0.25) eV respectively. Furthermore, this band at 10.2 eV shows six distinct peaks with an additional one barely resolved at 9.99 eV (Fig. 3a), which is the number expected for the J values of ^7F term. In addition, the splittings among the different J components are qualitatively as expected for Eu^+ by analogy with the ^7F_J manifold of Sm.[18b] The HeIα spectrum shows two additional peaks at 11.79 and 12.42 eV, and additional intensity around 13.4 eV. The former two peaks correspond to the $^{7,9}S$ and $^{7,9}D$ states of the configurations [$4f^7(^8S)7s$] and [$4f^7(^8S)6d$] respectively. The weak band at 13.4 eV shows some indication of resolvable peaks. Since no optical data are available for the many states that should fall in this high-energy region, the nature of this band is not entirely certain. Even though the NeI spectrum shows no indication of peaks above 11 eV, a more definitive conclusion is precluded by the poor collection efficiency of electrons at lower kinetic energy.

There are distinct differences in the relative peak intensities found in the HeIα and NeI spectra. The intensity ratio $^7S/^9S$ is quite different; namely, it is ~2/1 in the HeI spectrum and ~1/1 in the NeI case. The ratio in NeI is quite close to the statistical ratio 7/9, while that in HeI is unexpectedly larger. Secondly, the total relative intensity of the two $^{7,9}D$ peaks is much larger in HeI and that of the $^{7,9}P$ peaks is much smaller compared to those of the NeI counterparts.

In the HeI spectrum, the $^{7,9}S$ and ^9D states excited by HeIβ line, and the $^{7,9}S$ states by HeIγ are positively identified. It is important to note that the $^7S/^9S$ ratio continues to deviate from the statistical ratio at the HeIβ energy (it is 1.8/1) but returns to the expected value of 7/9 at the HeIγ energy. Furthermore, the ^9D intensity[25] is still larger in HeIβ relative to HeIα, while that in HeIγ is much smaller (cf Table III). The ^7D excited by the HeIβ line is however overlapped by the intense $^{7,9}S$ at 5.8 eV.

D. $Yb(4f^{14}6s^2;{}^1S)$

In contrast to the cases of Ba, Sm, and Eu, the HeI and NeI spectra of Yb , shown in Fig. 4, are very similar. Both spectra show three intense peaks at 6.25, 8.91, and 10.17 eV corresponding to the Yb^+ final states $(4f^{14}6s;{}^2S)$, $(4f^{13}6s^2;{}^2F_{7/2})$, and $(4f^{13}6s;{}^2F_{5/2})$ respectively. Three weak peaks at 9.27, 9.61, and 10.02 eV, which are better resolved in the NeI spectrum, are associated with the Yb^+ states $(4f^{14}5d;{}^2D_{5/2})$, $(4f^{14}6p;{}^2P_{1/2})$, and $(4f^{14}6p;{}^2P_{3/2})$. In addition, there are peaks at 9.82 eV, 10.42 eV, and a number of peaks above 11.6 eV; however, the nature of these weak peaks cannot be definitely determined.

IV. DISCUSSION

A. General Consideration of Correlation Effects

In a recent paper, we[5] reported the correlation satellites in the atomic photoelectron spectra of Group-IIA and Group-IIB elements. Considering their similar valence electronic structure (s^2), we expected the lanthanides to show similar correlation effects. Accordingly, the following discussion will follow closely, except as noted, the approach adopted earlier.[5]

Because the photo ion formed by removal of a 6s-electron might be approximated by a one-electron system, the contribution of FISCI to satellite structure should be small by analogy to H and He^+, for which CI is unnecessary. The importance of the CSCI contribution is more difficult to estimate, but it will be neglected on grounds that it is generally expected to be most significant near threshold and/or for ions with closely-spaced states of the same symmetry. Therefore for the 6s ionization in Ba and the lanthanides, we shall assume that only ISCI and possibly autoionization can lead to satellites of substantial intensity.

By analogy to the Group-II elements,[5] the ground states of the lanthanides can be approximated by ISCI as

$$\psi = a|6s^2;{}^1S\rangle + b|5d^2;{}^1S\rangle + c|6p^2;{}^1S\rangle + \ldots , \qquad (1)$$

where the [Xe] core and the 4f-electrons have been suppressed, and $a \gg b \sim c$. Consequently, the photoelectron spectra of the lanthanides will show, in addition to intense peaks due to the 6s ionic states, weak lines corresponding to states such as 5d, 6p etc. The intensities of the satellites depend upon the ISCI admixture coefficients as well

as the differential photoionization cross sections. The latter normally vary smoothly with photon energy, barring the existence of Cooper minimum and resonance,[26] and over a small span of energy, say 5 - 10 eV, an order of magnitude change in cross sections is normally not expected. Consequently, if the satellites are interpreted entirely in terms of ISCI, the shapes of the spectra excited by HeI and NeI radiation should reveal little difference. This was indeed observed in Ca and Sr,[5] for which the satellite intensities hardly changed relative to the main line in both HeI and NeI spectra.

Among the cases studied here, the spectra of Yb fall within the above expectation while those of Ba, Sm, and Eu showed differences too large to be explained in terms of ISCI alone. The unexpected features all appeared at the photon energies of HeI radiation (for Ba, at more energetic NeI lines as well) and can be summarized as follows. (1) The relative intensities of the satellites are far too large to be expected from ISCI considerations. This behavior is dramatized in the HeI spectrum of Ba (Fig. 1a) which showed a number of satellites with intensities comparable to the 6s main line. This trend is further continued at several photon energies close to the HeIα (21.22 eV) line. (2) The intensity ratios of the exchange multiplets of $Sm^+(4f^6 6s;\ ^{6,8}F)$ and $Eu^+(4f^7 6s;\ ^{7,9}S)$ deviate considerably from their respective statistical multiplicity ratios. This indicates that additional mechanisms must be present at HeI energies to account for the "anomalies". In contrast, all the NeI spectra are consistent with our simple picture of ISCI, and will be interpreted as such.

B. ISCI and Satellite Structure

Let us first discuss the NeI spectra. There are two points worth noting in going from Ba, Sm, Eu to Yb. First is the variation of satellite intensities across the series. To first approximation the satellite intensities may be estimated by the squares of the CI admixture coefficients, and the magnitude of the coefficients reflects the extent of ISCI. This approximation neglects the differences in photoionization cross sections, and its limitations have been discussed elsewhere.[5,27] Experimentally, the 5d intensities appear to decrease with increasing nuclear charge, while the variation of the 6p intensities is considerably less, except for Sm. This intensity trend may be understood qualitatively by a simple consideration of CI effects. The energy of the 5d ionic state increases from Ba to Yb much faster (cf Tables I - IV) than that of the 6p state. This suggests that the energy of the $5d^2(^1S)$ configuration should also increase faster than that of the $6p^2(^1S)$. This trend in energy should be reflected roughly in the CI admixture coefficients, and thus is consistent with the variation of satellite intensities. By contrast, the decrease in satellite intensities for Sm seems to conflict with the simple energy argument. We note, however, that Sm differs from the other three atoms in having one empty 4f-orbital.

Secondly, in the cases of Sm, Eu, and Yb, depending upon the mode of ionization, the resulting ionic states may be formed with two open shells. The question then arises whether the open shell originally present will remain unchanged, or to the same effect, which of the possible final ionic states derived from the same electronic configuration can be reached upon ionization. Let us first consider the

ionization of the outermost electron from Eu. Among the many possible states of the configurations $4f^7 6s$, $4f^7 5d$, and $4f^7 6p$, only $[4f^7(^8S)6s;^{7,9}S]$, $[4f^7(^8S)5d;^{7,9}D]$, and $[4f^7(^8S)6p;^{7,9}P]$ have been positvely detected. This suggests that the above states 'used up', within experimental error, the intensity derived from the admixed configurations $4f^7 6s^2$, $4f^7 5d^2$, and $4f^7 6p^2$ in the initial state. Furthermore, considering that the $[4f^7(^8S)5d^2(^1S);^1S]$ and $[4f^7(^8S)6p^2(^1S);^1S]$ states are most likely the major components in the ISCI expansion we can then conclude that hardly any recoupling within the $4f^7$ manifold occurred upon ionization. This is not surprising since the transition to the states $[4f^7(^8S)6s;^{7,9}S]$, $[4f^7(^8S)5d;^{7,9}D]$, and $@4f^7(^8S)6p;^{7,9}P]$ can be regarded as a 'one-electron' transition respectively from the ISCI components, and hence their cross sections should be much larger than those for all other states of $4f^7 6s$, $4f^7 5d$, and $4f^7 6p$. The corresponding situation in Sm is not as clear-cut, because the satellite intensities are too low to allow for a meaningful discussion. Nevertheless, it is clear that the 4f shell remained unchanged in the $4f^6 6s$ manifold.

Next we consider the situation in which a 4f electron is ionized. Besides the $(4f)^{-1}$ primary lines, satellite states caused by ISCI may also be observed. Assuming no recoupling in the open shell, the satellites most likely to be found should be formed from the configurations $Sm^+[4f^5 5d^2(^1S)]$, $Sm^+[4f^5 6p^2(^1S)]$, $Eu^+[4f^6 5d^2(^1S)]$, $Eu^+[4f^6 6p^2(^1S)]$, $Yb^+[4f^{13} 5d^2(^1S)]$, and $Yb^+(4f^{13} 6p^2(^1S)]$, where the coupling within the $4f^n$ shell and the total state designation are identical and are dictated by the initial state and the selection rules. To our knowledge, the energies of these excited ionic states have not been determined, thus making their detection in the spectra difficult. They may, however,

account for some of the unassigned lines in the Sm, Eu, and Yb spectra. We note that this subject arose in the study of Hg by Berkowitz et al.[9] The wavefunction for the ground state of Hg can be approximated as[5,9]

$$\psi(^1S) = a|5d^{10}6s^2;^1S\rangle + b|5d^{10}6p^2;^1S\rangle + \ldots . \qquad (2)$$

Removal of 5d-electron from the second configuration results in the configuration $5d^96p^2$, which consists of two open shells. In light of the above discussion, it seems that $6p^2$ would remain coupled to ^1S and only the Hg^+ states $[5d^96p^2(^1S);^2D_{5/2}]$ and $[5p^96p^2(^1S);^2D_{3/2}]$ would contribute significantly to the electron distribution around 27.5 - 30 eV observed in the HeII spectrum (contribution from $5d^96s7s$ manifold is also possible).[9] This interpretation is consistent with the fact that the electron distribution in question appears to consist mainly of two lines at 27.8 and 29.7 eV, whose separation is close to the spin-orbit splitting 1.86 eV between $[5d^96s^2;^2D_{3/2,\ 5/2}]$. Finally, we point out that relativistic effects may cause further mixing of configurations, and especially for Sm^+ and Eu^+, this mixing may be quite important.

C. Autoionization and Satellite Structure

We now turn to the unexpected features found in the HeI spectra of Ba, Sm, and Eu. The dramatic HeI photoelectron spectrum of Ba has recently attracted a great deal of interest.[10-14] Autoionization, together with other mechanisms,[11-14] has been proposed to explain the unusual spectrum. We shall offer evidence that autoionization is the main cause of the peculiar spectrum, and furthermore, that the same mechanism is responsible for the unexpected behavior of the HeI spectra of Sm and Eu.

Heuristically, autoionization may be visualized as a two-step process. The first step involves a resonant transition to a Rydberg-type discrete state, which then decays into different continuum states, giving off free electrons with kinetic energies that label the final ionic-state energies. Autoionization arises because of the interaction between the discrete state and various continuum states. This interaction and the resulting mixing of states has been treated by Fano[3] using the CI model. In this picture, the rather large oscillator strength of the resonant transition is shared among the various coupling channels, and the probability of decaying via the individual channels is in first approximation proportional to the amount of respective mixing. Therefore, if autoionization occurs, the photoelectron spectrum will be strongly affected because each photoelectron line will derive its intensity from both direct and indirect (autoionization) ionization. The exact appearance of the resulting spectrum could be predicted only by a detailed theoretical analysis. Such an analysis is not presented here. Consequently, our discussion has to be qualitative in nature.

In general, unequivocal evidence of autoionization is frequently found in absorption spectra by observing a large absorption intensity, a broad linewidth, and an asymmetric line shape. The absorption spectrum of Ba in the energy region relevant to the photoemission work has recently been reported.[15,16] In the 19 - 25 eV region this spectrum showed a large number of strong, broad absorption lines, and indeed the lines are so densely spaced as to simulate a molecular band-type absorption. This is understandable considering that the binding energies

of the $5p_{3/2}$ and $5p_{1/2}$ electrons lie at 22.7 and 24.8 eV, and thus the Rydberg states converging to these two thresholds are expected to fill the energy interval in question quite closely. Considering the rather effective screening of the 4f-electrons, the $(5p)^{-1}$ thresholds for Sm and Eu are expected to lie not far above those of Ba. Therefore in the energy region near the HeI lines, a large number of closely-spaced Rydberg states is anticipated for Sm and Eu as well. This expectation is indeed substantiated by the absorption spectra of Sm and Eu recently recorded by Connerade et al.[28] In accordance with the foregoing energy considerations, it is quite natural that autoionization in Sm and Eu should occur at HeI energies. At the energy of NeI lines, the absorption spectra of Ba,[15,16] Sm,[28] and Eu[28] showed no absorption lines, whereas for Yb, the 5p threshold moves up high enough in energy that the absorption spectrum[28] showed no appreciable absorption around both the HeI and NeI energies. This supports our interpretation of the NeI spectra of all atoms and the HeI spectrum of Yb in terms of ISCI alone. In addition to the evidence from absorption spectra and from energy considerations, further identification of autoionization is provided by comparing the photoelectron spectra excited with photons of different energies. In general, spectra in which autoionization occurs show drastic deviations from expectations based on initial-state configuration interaction alone. By combining the above considerations, we believe that autoionization has been detected in the HeI photoelectron spectra of Ba, Sm, and Eu, as discussed below.

D. Autoionization in Ba

The remarkable contrast between the HeI and NeI spectra of Ba, together with the evidence from absorption[15,16] and previous photoemission work,[10-13] firmly establishes that autoionization processes are occurring in the HeIα spectrum. The HeIα line overlaps a 5p absorption line such that a Rydberg state is resonantly excited. This state is mixed, through CI, with a number of continuum states such as $[(Ba^{+}5p^{6}n\ell)(\varepsilon\ell')]^{o}_{J=1}$, $[(Ba^{+}5p^{5}n\ell n'\ell')(\varepsilon\ell'')]^{o}_{J=1}$, and $[(Ba^{++}5p^{6})(\varepsilon\ell')(\varepsilon\ell'')]^{o}_{J=1}$. Resonant excitation and autoionization of this state thus gives rise to the various peculiar features observed in the HeI spectrum. This process is described schematically in Fig. 5. The admixed $(Ba^{+}5p^{6}n\ell)(\varepsilon\ell')$ states autoionize directly to yield the $Ba^{+}(5p^{6}n\ell)$ lines, which are detected as peaks through the kinetic energies of the continuum electrons. $(Ba^{++}5p^{6})(\varepsilon\ell)(\varepsilon\ell')$ decays to the Ba^{++} $(5p^{6})$ state by giving off two continuum electrons, yielding a continuous electron distribution at energies above the Ba^{++} threshold (15.215 eV). The $(Ba^{+}5p^{5}n\ell n'\ell')(\varepsilon\ell'')$ manifold first autoionizes to form the highly-excited $(Ba^{+}5p^{5}n\ell n'\ell')$ states, yielding the three peaks at very low kinetic energies; i.e., at ca. 0.1 eV, detected by Hotop and Mahr.[12] These resulting Ba^{+} states can undergo further Auger transitions to the Ba^{++} $(5p^{6})$ state, with the corresponding Auger electrons detected at ca. 5.9 eV (peaks 1,2, and 3 in Fig. 1a). The energetics of this two-step autoionization-Auger process were discussed by Hansen,[14] who also suggested that the same process is responsible for double ionization

being more probable than single ionization.[10]

The HeIα spectrum of Ba consists of contributions from direct ionization as well. The respective contributions due to direct and indirect (autoionization) ionization cannot be distinguished quantitatively. We note this could be accomplished by using a tunable light source such as synchrotron radiation. Some qualitative deductions may however be reached by comparing the HeI and NeI spectra. The intensities of all lines more energetic than the Ba^{+} 6p peaks must come almost exclusively from autoionization, as must more than 95% of the 5d and 6p peak intensities. The predominant part of the intensity of even the 6s states also comes from autoionization, as suggested by its relatively small intensity at the HeIβ energy. The 6s intensity is only 0.6% (Table 1) at the HeIβ energy relative to that at the HeIα energy, as opposed to the ~5% flux of HeIβ radiation usually found in the photon source (Table 5).

The photoelectron lines (labelled S in Fig. 1a) excited by HeIβ radiation again shows two unusual features that indicate the occurrence of autoionization. First, the 5d/6s intensity ratio is ~ 3/1 which is not expected from the ISCI model. Next, the $5d_{5/2}/5d_{3/2}$ ratio is ~ 1/1.1, as opposed to the multiplicity ratio 5/3. It is worthwhile noting that the multiplicty ratios are observed rather well in the HeI spectrum (cf Table 1). As suggested by Brehm and Höfler,[11] the peaks 4 - 10 in Fig. 1a may be assigned to the higher Rydberg states converging to the Ba^{++} threshold. If this is the case, the sudden increase in the intensities of these lines seems unexpected judging from the trend of other satellite intensities. In view of our finding

that autoionization occurs at the HeIβ line energy, it is likely that part of the electron intensity between peaks 4 - 10 arises in the same way as do peaks 1 - 3, i.e., via a two-step autoionization-Auger process. Unfortunately, the corresponding autoionizing electrons were not detected due to poor analyzer transmission at low energies; otherwise the above assignment could be tested.

Autoionization also appears to occur at the various NeI line energies listed as peaks S_1, S_2, S_3 in Table 5 and Fig. 1b. This is suggested by the high photoelectron line intensities relative to the relative radiation line intensities in the usual photon flux from NeI sources, as well as the large intensity ratio of the 5d to 6s states (cf Tables 1 and 5). Furthermore, these NeI lines lie right at the seemingly continuous absorption region of the Ba absorption spectrum.[15,16] The autoionizing states involved at the NeI line energies do not seem to undergo a two-step ionization, as there is no indication for the existence of the corresponding electron lines in the spectrum (Fig. 1b)

E. Autoionization of Sm and Eu

The differences between the HeI and NeI spectra of Sm and Eu have been pointed out in Section IIIB and IIIC respectively. Following the reasoning presented above, these differences can now be understood in terms of autoionization processes. Therefore, autoionization is suggested by the spectra to occur at the HeIα line energy for Sm, and at HeIα and HeIβ energies for Eu. For all three cases, the intensity ratios measured from spectra of the multiplets of the ground ionic states deviate considerably from the expected statistical ratio (cf section IIIB and IIIC): a phenomenon also observed for the 5d doublets of Ba^+

excited by the HeIβ line. Intuitively, this large deviation is quite unexpected, considering the similarity of the states involved, but somehow it appears to reflect the subtlety of the interaction in the final states.

V. CONCLUSIONS

Satellite lines have been observed in both HeI and NeI photoelectron spectra of Ba, Sm, Eu, and Yb. The lines have been interpreted in terms of initial-state configuration interaction and autoionization in the final state. By using the different rare gas resonance lines, it was possible to selectively excite certain autoionizing levels, and subsequently identify the satellite structure due to autoionization. Photoelectron spectra showing autoionization were found to contain a great deal of information about the nature and extent of the interaction between the discrete level and the individual continuum channels. The sensitivity of photoelectron spectra toward this coupling is far superior to that of natural line widths, absorption line profiles, etc. revealed in absorption spectra, because the photoelectron channel adds a new dimension of information. Therefore it is anticipated that photoelectron spectroscopy, carried out with a continuously tunable photon source such as synchrotron radiation, will become a powerful method of studying electron correlation in both initial and final states.

ACKNOWLEDGEMENTS

We are indebted to Miss Geri Richmond for experimental assistance, to Dr. J. P. Connerade for sending us the absorption spectra of metal vapors prior to publication, and to Mr. R. S. Williams for help with the relativistic Hartree-Fock calculation.

REFERENCES AND FOOTNOTES

1. R. L. Martin and D. A. Shirley, J. Chem. Phys. 64, 3685 (1976).

2. S. T. Manson, J. Elect. Spect. 9, 21 (1976).

3. U. Fano, Phys. Rev. 124, 1866 (1961).

4. R. L. Martin and D. A. Shirley, Phys. Rev. 13, 1475 (1976).

5. S. Süzer, S.-T. Lee, and D. A. Shirley, Phys. Rev. 13, 1842 (1976).

6. S. Süzer, M. S. Banna, and D. A. Shirley, J. Chem. Phys. 63, 3473 (1975).

7. S. Süzer, S.-T. Lee, and D. A. Shirley, J. Chem. Phys. 65, 412 (1976).

8. S. Süzer and D. A. Shirley, J. Chem. Phys. 61, 2481 (1974).

9. J. Berkowitz, J. L. Dehmer, Y. K. Kim, and J. P. Desclaux, J. Chem. Phys. 61, 2556 (1974).

10. B. Brehm and A. Bucher, Int. J. Mass Spectrom. Ion Phys. 15, 463 (1974).

11. B. Brehm and K. Höfler, Int. J. Mass Spectrom. Ion Phys. 17, 371 (1975).

12. H. Hotop and D. Mahr, J. Phys. B8, L301 (1975).

13. U. Fano, Comments On At. and Mol. Phys. 4, 119 (1973).

14. J. E. Hansen, J. Phys. B8, L403 (1975).

15. J. P. Connerade, M.W.D. Mansfield, K. Thimm, and D. Tracy, VUV Radiation Physics, ed. by E. E. Koch, R. Haensel, and C. Kunz (Pergamon, Vieweg, 1974), p. 243.

16. D. L. Ederer, T. B. Lucatorto, and E. B. Salomon, VUV Radiation Physics, ed. by E. E. Koch, R. Haensel, and C. Kunz (Pergamon, Vieweg, 1974), p. 245.

17. R. G. Newburgh, L. Heroux, and H. E. Hinteregger, App. Optics 1, 733 (1962).

18. (a) Ba –C. E. Moore, Natl. Bur. Stand. (U.S.A.) Circ. 467, Vol. 3 (1962); (b) Sm — J. Blaise, C. Morillon, M-G Schweighofer, and J. Verges, Spect. Acta 24B, 405 (1962); W. Albertson, Astrophys. J. 84, 26 (1936). (c) Eu — A. C. Parr, J. Chem. Phys. 54, 3161 (1971); H. N. Russell, W. Albertson, and D. N. Davis, Phys. Rev. 60, 641 (1941). (d) Yb — V. Kaufman and J. Sugar, J. Opt. Soc. Amer. 63, 1168 (1973); W. F. Meggers, J. Res. NBS, 71A, 396 (1967); A. C. Parr and F. A. Elder, J. Chem. Phys. 49, 2665 (1968).

19. J. P. Desclaux, Comp. Phys. Comm. 9, 31 (1975).

20. D. A. Shirley, R. L. Martin, B. E. Mills, S. Süzer, S.-T. Lee, E. Matthias, and R. A. Rosenberg, Proc. 2nd Int. Conf. on Inner Shell Ionization Phenomena, Freiberg, Germany, March 29 - April 2, 1976; S.-T. Lee, R. A. Rosenberg, E. Matthias, and D. A.Shirley, to be published.

21. P. A. Cox and F. A. Orchard, Chem. Phys. Lett. 7, 273 (1970); P. A. Cox, S. Evans, and F. A. Orchard, ibid, 13, 386 (1972).

22. C. W. Nielson and G. F. Koster, Spectroscopic Coefficients for the p^n, d^n, and f^n Configurations, The M.I.T. Press (1963).

23. Leo Brewer, J. Opt. Soc. Amer. 61, 1666 (1971).

24. W. T. Carnall, P. R. Fields, and K. Rajnak, J. Chem. Phys. 49, 4424 (1968).

25. The ionization of He by HeII (40.8 eV) line falls close to the ^9D signal, but its contribution to the intensity is estimated to be less than a few per cent.

26. J. W. Cooper, Phys. Rev. Lett. 13, 762 (1964); U. Fano and J. W. Cooper, Rev. Mod. Phys. 40, 441 (1968).

27. J. E. Hansen, private communication and to be published.

28. J. P. Connerade, private communication.

TABLE I. Observed states of Ba^+ and relative peak intensities in HeI and NeI spectra.

Ba^+ state[a]		Binding[b] energy (eV)	Optical[c] value (eV)	Intensity[d] HeI	Intensity[e] NeI
6s	$^2S_{1/2}$	5.211	5.211	100; 0.6	100; 1.6; 5.4; 0.8
5d	$^2D_{3/2}$	5.81	5.816	72; 0.9	22; 2.2;
	$^2D_{5/2}$	5.91	5.915	160; 0.8	5.0; ——
6p	$^2P_{1/2}$	7.72	7.723	36	1.5
	$^2P_{3/2}$	7.93	7.933	63	3.2
7s	$^2S_{1/2}$	10.46	10.463	38	0.7
6d	$^2D_{5/2,3/2}$	10.92	10.908; 10.934	108	0.7
4f	$^2F_{7/2,5/2}$	11.20	11.195; 11.222	19	0.5
7p	$^2P_{1/2}$	11.33	11.335	15	
	$^2P_{3/2}$	11.40	11.412	33	
5f	$^2F_{5/2,3/2}$	12.34	12.327; 12.357	28	

TABLE I. (con't)

Ba^+ state[a]		Binding[b] energy (eV)	Optical[c] value (eV)	Intensity[d] HeI	Intensity[e] NeI
8s	$^2S_{1/2}$	12.40	12.405	47	
7d	$^2D_{5/2,3/2}$	12.63	12.626; 12.637	37	
8p	$^2P_{3/2,1/2}$	12.84	12.816; 12.853	20	
5g	$^2G_{9/2,7/2}$	13.02	13.026	11	
6f	$^2F_{7/2,5/2}$	13.22	12.220; 12.233	10	
9s	$^2S_{1/2}$	13.35	13.355	5	
8d	$^2D_{5/2,3/2}$	13 48	13.478; 13.484	7	
9p	$^2P_{3/2,1/2}$	13.61	(13.583; 13.603)	12	
6g	$^2G_{9/2,7/2}$	13.69	13.695	13	
7f	$^2F_{7/2,5/2}$	13.79	13.792; 13.798	3	

TABLE I. (con't)

Ba^+ state[a]		Binding[b] energy (eV)	Optical[c] value (eV)	Intensity[d] HeI	Intensity[e] NeI
10s	$^2S_{1/2}$	13.89	13.892	2	
9d	$^2D_{5/2,3/2}$	13.96	13.967; 13.971	2	
10p	$^2P_{3/2,1/2}$	14.04	(14.031; 14.045)	4	
7g	$^2G_{9/2,7/2}$	14.10	14.099	5	
(11s)	10	14.22	(14.226)	0.65	
(11p)	9	14.32	(14.317,14.325)	0.40	
(12s)	8	14.45	(14.447)	0.28	
	7	14.56		13	
	6	14.66		2	
	5	14.77		3	

TABLE I. (con't)

Ba^+ state[a]	Binding energy[b] (eV)	Optical value[c] (ev)	Intensity HeI[d]	Intensity NeI[e]
4	15.12		44	
3	15.28	15.283	291	
2	15.37	15.366	221	
1	15.42	15.420	81	

a. The [Xe] core has been suppressed in this notation. Peaks 1 - 3 are Auger transitions. For other numbered states, the assignment is not final; see text.

b. The error limit is less than 10 meV.

c. Optical binding energies were obtained from ref. 18a. The values in parenthesis are binding energies estimated from the Rydberg formula, and those for states 1 - 3 are from ref. 12.

d. Intensities are corrected for $\Delta E/E$ dependence and referenced to the Ba^+6s/HeI_α line. Where there are two entries, the first is from the HeI_α and the second from the HeI_β spectrum.

e. Intensities are corrected for $\Delta E/E$ dependence and referenced to Ba^+6s/NeI line. Where there is more than one entry, the first value is from NeI main line, and the others are from NeI S_3, S_2, and S_1 satellite lines.

TABLE II. Observed states of Sm^+ and relative peak intensities in HeI and NeI spectra.

Sm^+ state[a]	Binding[b] energy (eV)	Optical value (eV)	Intensity[e] HeI	Intensity[e] NeI
$4f^6 6s$ ^8F	5.64(2)	5.63[c]	27	100
^6F	5.80(2)	5.82[c]	100	100
$4f^6 5d$	6.61(2)	6.52-8.19[c]	7	4
	6.94(2)		18	4
	7.39(2)		8	——
	7.70(2)		8	——
	7.90(2)		13	——
$4f^6 6p$	8.4 (1)	>8.27[c]	20	<10
$4f^5 6s^2$ ^6H	8.8 (1)	9.0 [d]	76	140
^6F	9.6 (1)	9.7 [d]	35	77
^6P	11.9 (1)	11.7 [d]	39	64

a. The [Xe] core has been suppressed. The particular states of the ($4f^6 5d$) and ($4f^6 6p$) configurations cannot be identified, nor are the J values for all the states.

b. The error is listed in parenthesis. The binding energies for broad bands are the vertical values.

c. From ref. 18b. The values for ^6F and ^8F correspond to the transitions $Sm(^7F_o) \rightarrow Sm^+(^8F_{1/2})$ and $Sm^+(^6F_{1/2})$ respectively.

d. The values were estimated from refs. 23 and 24 (cf. text), and are the weighted centers of the individual terms. Ref. 23 gave $^6H_{5/2}$ at (8.61 ± 0.25) eV.

e. The intensities are corrected for the $\Delta E/E$ dependence of this type of spectrometer.

TABLE III. Observed states of Eu^+ and relative peak intensities in HeI and NeI spectra.

Eu^+ state[a]		Binding[b] energy (eV)	Optical[c] value (eV)	Intensity[d] HeI	Intensity[d] NeI
$4f^7 6s$	$^9S_4$	5.67	5.670	52; 4.5; 1.9	95
	$^7S_3$	5.88	5.877	100; 8.1; 1.5	100
$4f^7 5d$	$^9D_{2,3,4,5,6}$	6.96	6.900 - 7.049	26; 9.8; 0.7	12
	$^7D_{1,2,3,4,5}$	7.77	7.760 - 7.817	32	10
$4f^7 6p$	$^9P_{3,4}$	8.67(5)	8.617; 8.670	3	7
	$^9P_5$	8.92	8.914	0.6	2
	$^9P_{4,3,2}$	9.04	8.997; 9.029; 9.048	2	4
$4f^6 6s^2$	$^7F_0$	9.99(3)	———		
	$^7F_1$	10.07	———		
	$^7F_2$	10.15	———		
	$^7F_3$	10.25	———	114	226
	$^7F_4$	10.37	———		
	$^7F_5$	10.46	———		
	$^7F_6$	10.55	———		

TABLE III. (con't)

Eu^+ state[a]	Binding[b] energy (eV)	Optical[c] value (eV)	Intensity[d] HeI	Intensity[d] NeI
$4f^7 7s$ $^9S_4$; $^7S_3$	11.79(3)	11.761; 11.825	2	——
$4f^7 6d$ ^9D ; ^7D	12.42	12.399 - 12.438	1	——

a. The [Xe] core has been suppressed.

b. The error limit is 20 meV except as listed in parenthesis. The binding energies for broad bands are the vertical ones.

c. From ref. 18C.

d. The intensities are corrected for the $\Delta E/E$ dependence and referenced to the $^7S_3$ line. Where there are three entries in the HeI column, they are from HeIα, HeIβ, and HeIγ spectra respectively.

TABLE IV. Observed states of Yb^+ and relative peak intensities in HeI and NeI spectra

Yb^+ state[a]	Binding[b] energy (eV)	Optical[c] value (eV)	Intensity[d] HeI	Intensity[d] NeI
$4f^{14}6s\ {}^2S_{1/2}$	6.25	6.254	100	100
$4f^{14}5d\ {}^2D_{5/2}$	9.2	9.271	6	10
$4f^{13}6s^2\ {}^2F_{1/2}$	8.91	8.910	180	281
$^2F_{5/2}$	10.17	10.168	95	135
$4f^{14}6p\ {}^2P_{1/2}$	9.61	9.609	3	3
$^2P_{3/2}$	10.02	10.022	5	5
——	9.82		2	6
——	11.77		7	2
——	12.37		8	9
——	13.53		11	12
——	14.68		4	——

a. The [Xe] core has been suppressed. Some states have not been identified.

b. The error limit is 20 meV.

c. The binding energies are from ref. 18d.

d. The intensities are corrected for $\Delta E/E$ dependence and referenced to the Yb^+6s line.

TABLE V. The energies and relative line intensities of the HeI and NeI resonance radiation spectra

Source	Excited state	Designation	Wavelength (Å)[a]	Energy (eV)	Relative intensity[b]
Helium capillary discharge	2^1P_1	HeIα	584.334	21.2175	100
	3^1P_1	HeIβ	537.030	23.0864	4.5(1.0)
	4^1P_1	HeIγ	522.213	23.7415	0.6(0.2)
Neon capillary discharge	$3s[3/2]^\circ_1$	NeI	743.718	16.6704	27(5)
	$3s'[1/2]^\circ_1$	doublet	735.895	16.8476	100
	$4s[3/2]^\circ_1$	S_3	629.74	19.688	0.5(0.2)
	$4s'[1/2]^\circ_1$		626.82	19.779	
	$3d[1/2]^\circ_1$	S_2	619.10	20.026	0.2(0.1)
	$3d[3/2]^\circ_1$		618.67	20.040	
	$3d'[3/2]^\circ_1$		615.63	20.139	

TABLE V. (con't)

Source	Excited state	Designation	Wavelength (Å)[a]	Energy (eV)	Relative intensity[b]
	$5s[3/2]^\circ_1$		602.73	20.570	
	$5s'[1/2]^\circ_1$		600.01	20.663	
	$4d[1/2]^\circ_1$	S_1	598.88	20.702	0.1(0.1)
	$4d[3/2]^\circ_1$		598.68	20.709	
	$4d'[3/2]^\circ_1$		595.92	20.805	
	$6s[3/2]^\circ_1$		591.82	20.949	
	$6s'[3/2]^\circ_1$		589.18	21.043	
	$5d[1/2]^\circ_1$	S_0	590.02	21.013	0.03(0.03)
	$5d[3/2]^\circ_1$		589.91	21.017	
	$5d'[3/2]^\circ_1$		587.23	21.113	

a. Reference 18a.

b. The relative intensity was determined by the Xe ^2P doublet. The values in parenthesis are the probable errors, predominantly due to intensity fluctuations in the source.

FIGURE CAPTIONS

Fig. 1 , Photoelectron spectra of Ba^+. (a) Excited by HeI lines. The peaks marked S are due to ionization by the HeIβ line. (b) Excited by NeI lines. The peaks marked S_1, S_2, and S_3 are due to ionization by the more energetic NeI satellite lines, and those starred are believed to be Auger peaks arising from excitation by the plasma electrons from the lamp and/or NeII radiation. In both spectra, the peaks marked I arise from elastically scattered electrons.

Fig. 2 Photoelectron spectra of Sm^+. (a) Excited by HeI line. The vertical bars are the estimated positions and intensities of the ^6H, ^6F, and ^6P terms of the ($4f^5 6s^2$) configuration (see text). (b) Excited by NeI line. The nature of the band at 10.5 eV is not known.

Fig. 3. Photoelectron spectra of Eu^+. (a) Excited by HeI lines. The lines marked S_β and S_γ are due to ionization by HeIβ and HeIγ lines. (b) Excited by NeI line. In both spectra, the lines marked I are elastically scattered electrons.

Fig. 4. Photoelectron spectra of Yb^+. (a) Excited by HeI lines. The lines marked S are due to ionization by HeIβ line. (b) Excited by NeI line. In both spectra, the lines marked I are elastically scattered electrons.

FIGURE CAPTIONS

Fig. 5. Energy diagram illustrating the autoionization process of Ba at HeIα energy. The 5p thresholds are from this work and the energy of ($5p^6 6s5d$) is from ref. 12. All other energy levels are from ref. 18a.

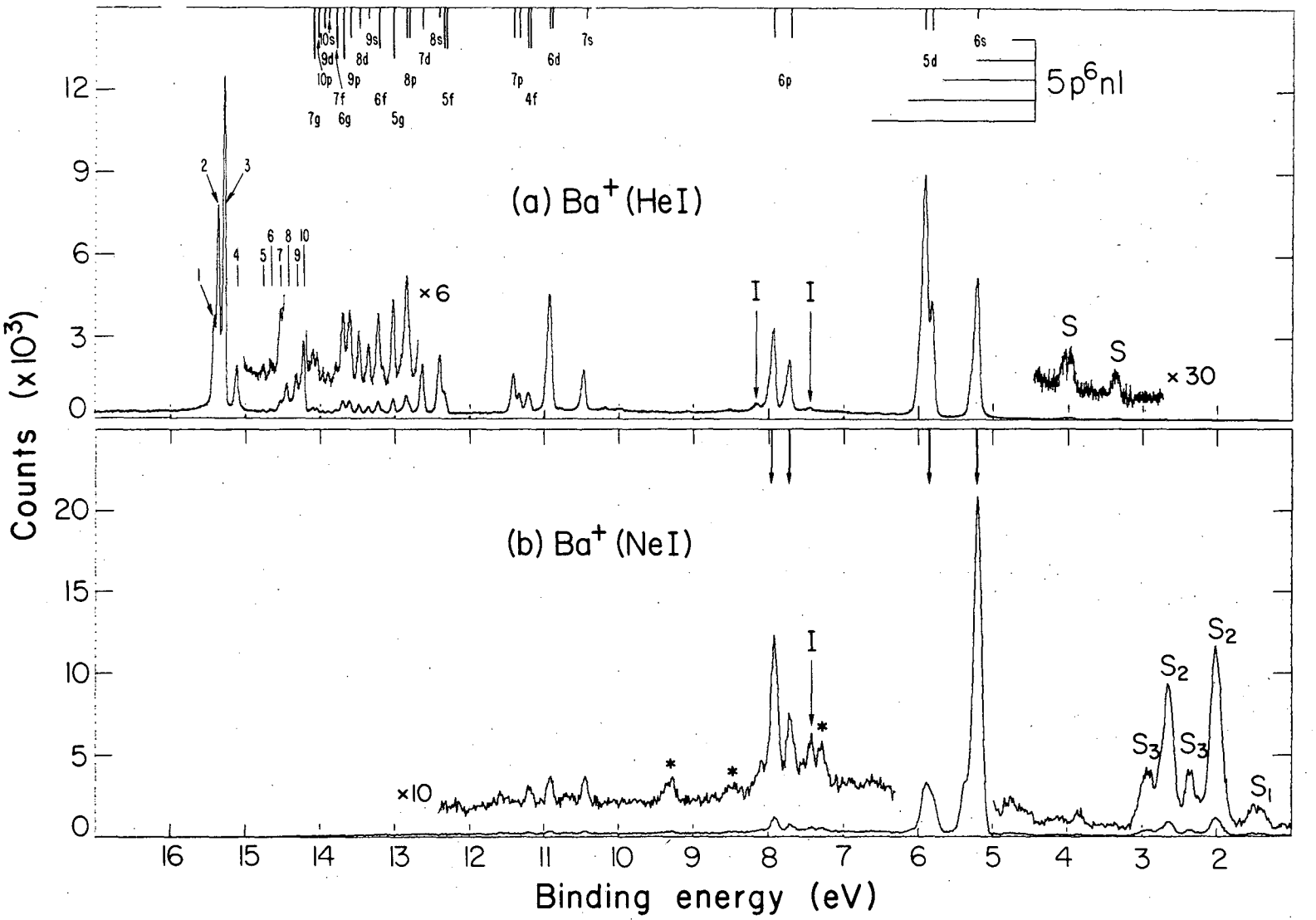
(a) Ba+ (HeI)
(b) Ba+ (NeI)
5p6nl
Counts (x10^3)
Binding energy (eV)
XBL 763-2444A

Fig. 1

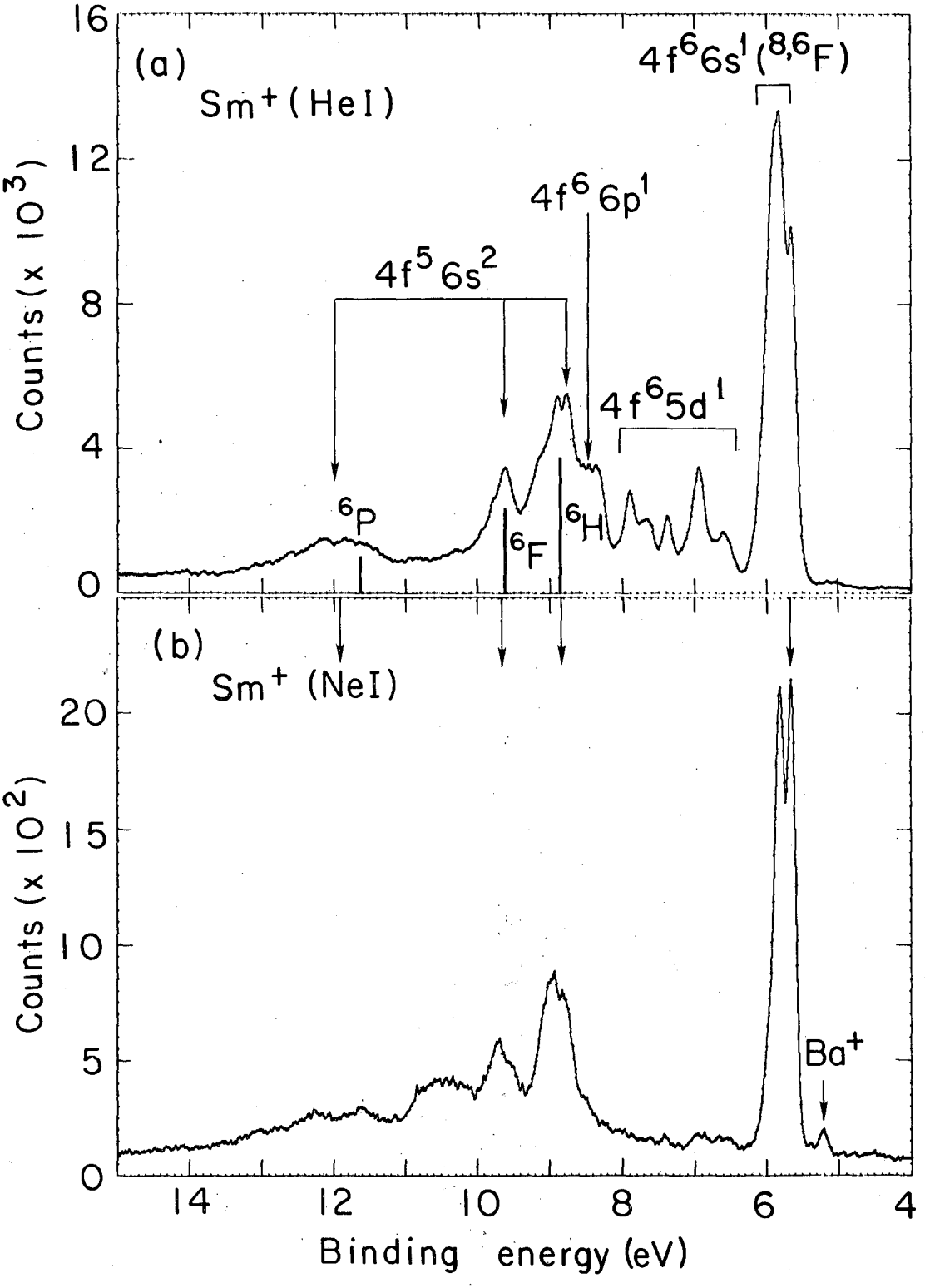

XBL 767 3238 A

Fig. 2

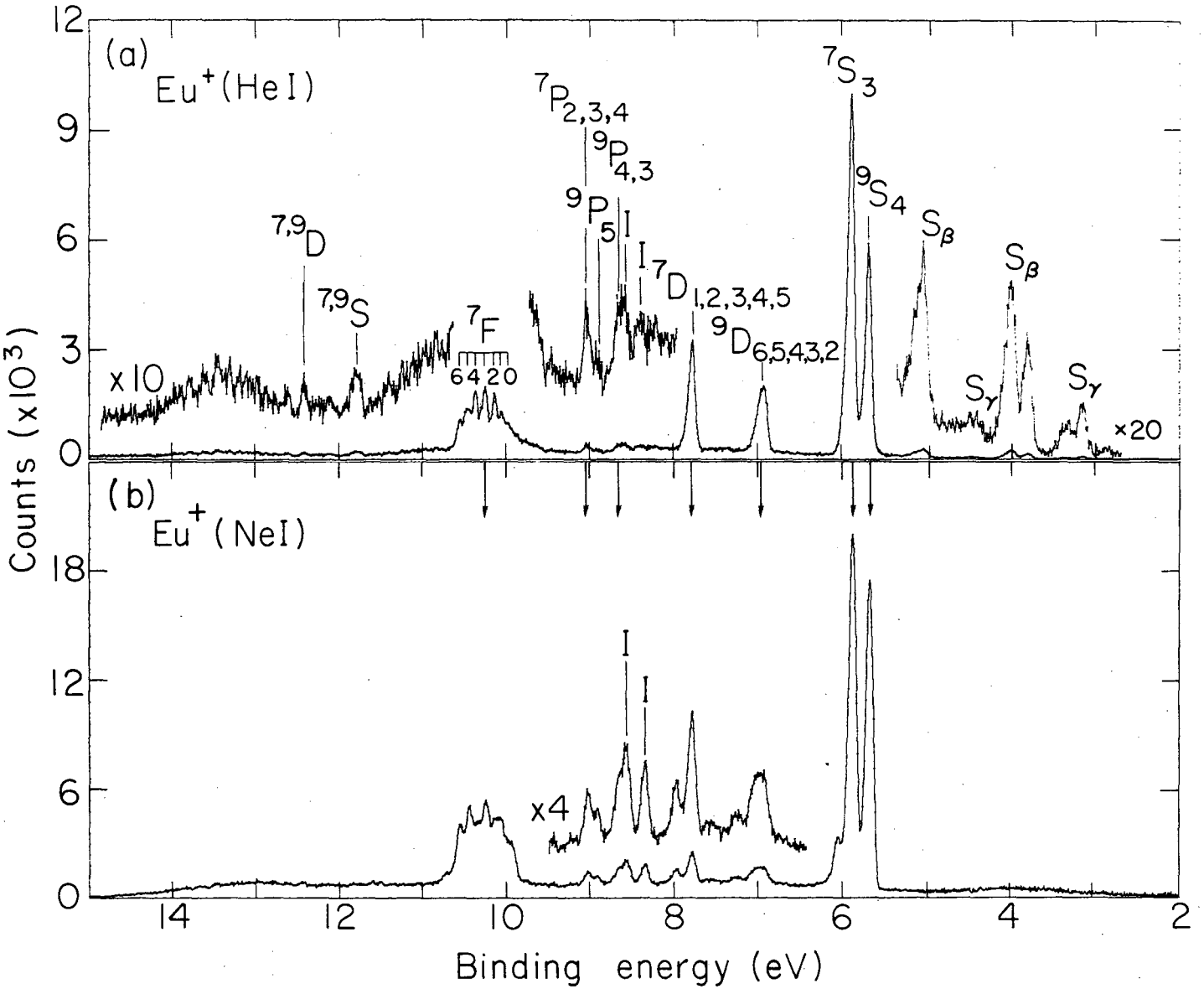

XBL 7512-9596 A

Fig. 3

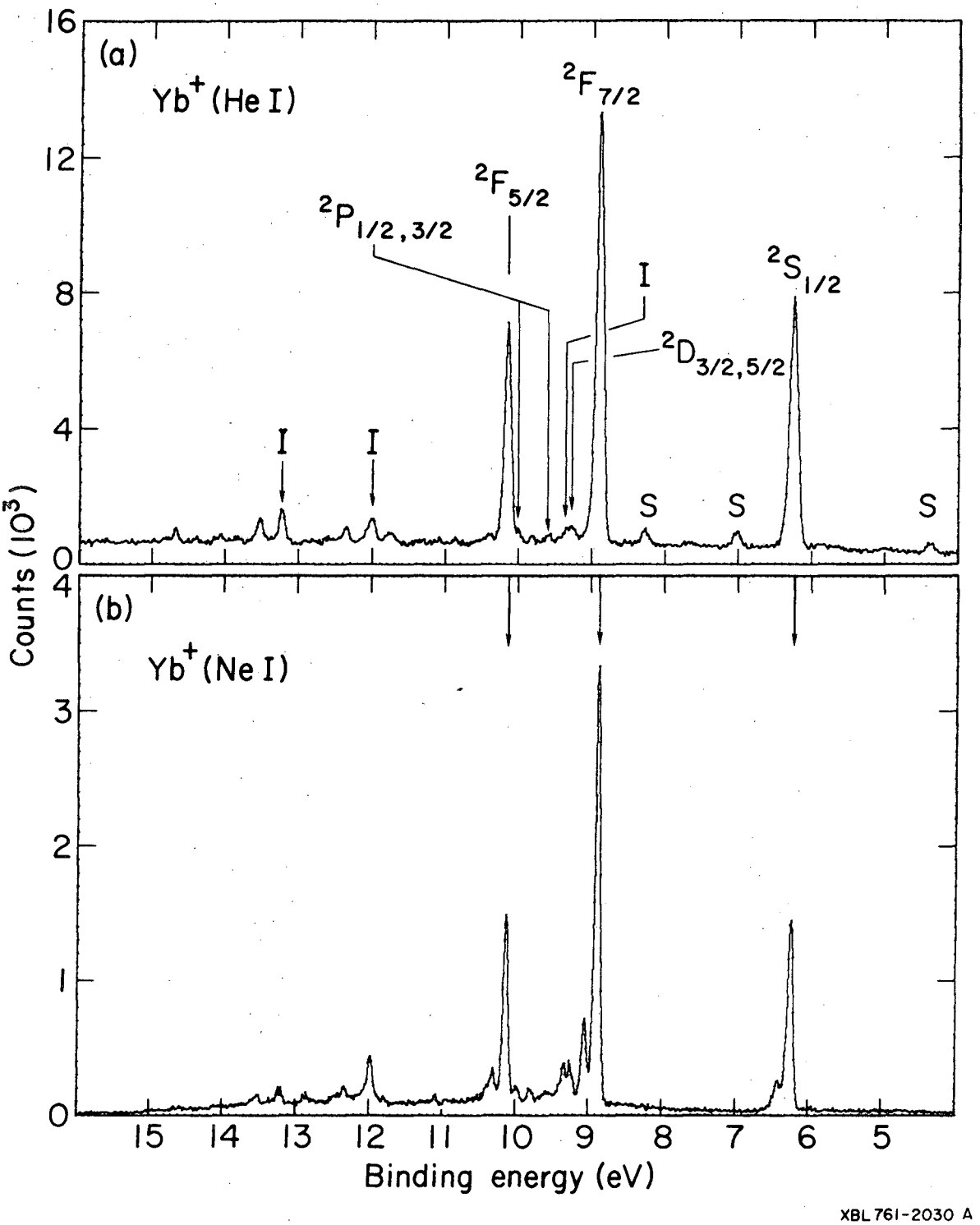

Fig. 4

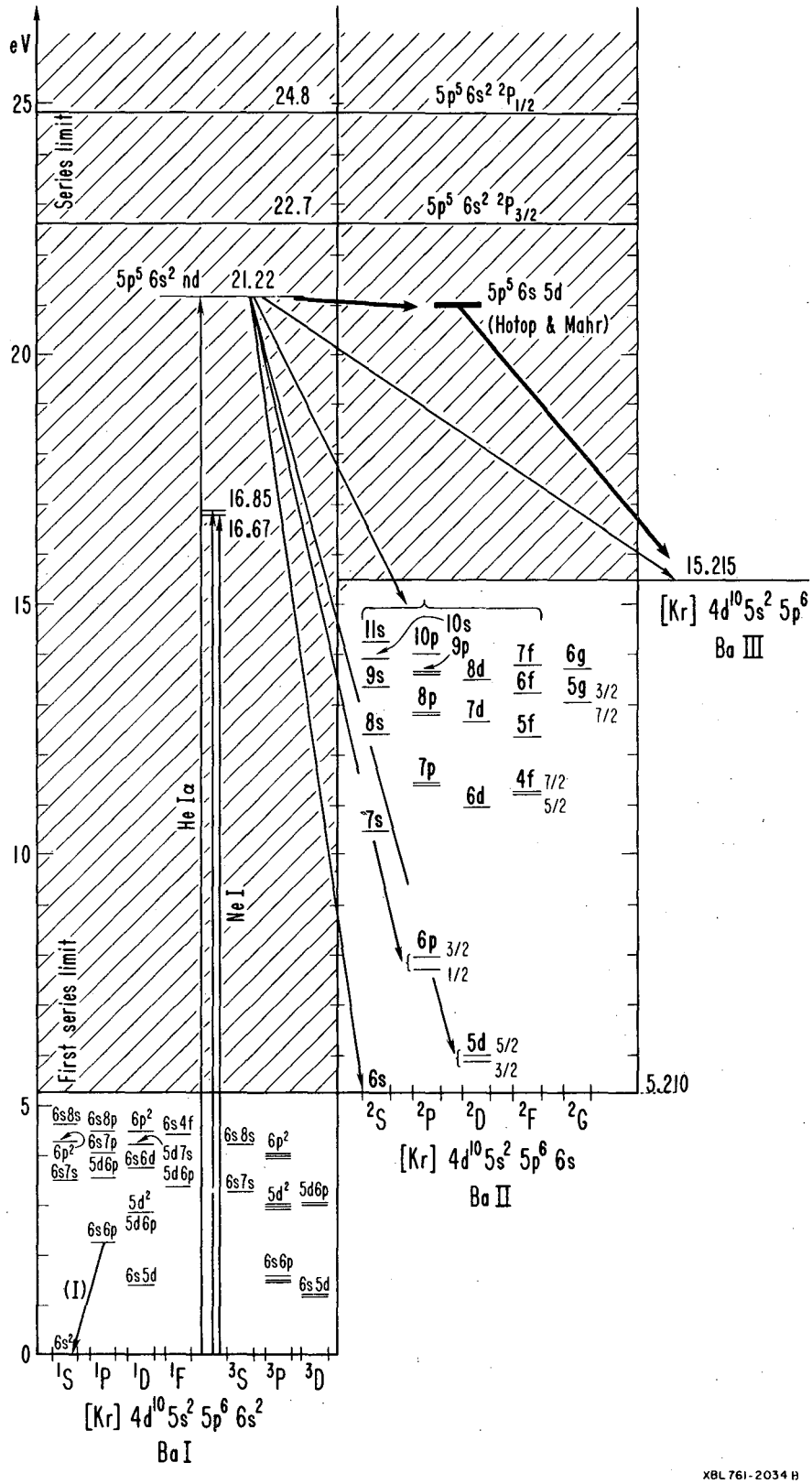
eV
25
20
15
10
5
0
24.8
$5p^5\,6s^2\,{}^2P_{1/2}$
Series limit
22.7
$5p^5\,6s^2\,{}^2P_{3/2}$
$5p^5\,6s\,nd$
21.22
$5p^5\,6s\,5d$
(Hotop & Mahr)
16.85
16.67
15.215
$[Kr]\,4d^{10}5s^2\,5p^6$
Ba III
He Ia
Ne I
First series limit
11s
10s
10p
9p
8d
7f
6g
9s
8p
7d
6f
5g 3/2
7/2
8s
5f
7p
6d
4f 7/2
5/2
7s
6p 3/2
1/2
5d 5/2
3/2
6s
5.210
^2S ^2P ^2D ^2F ^2G
$[Kr]\,4d^{10}5s^2\,5p^6\,6s$
Ba II
6s8s
6s8p
$6p^2$
6s4f
$6p^2$
6s7p
6s7s
6s6d
5d7s
5d6p
5d6p
$5d^2$
5d6p
6s6p
(I)
6s5d
$6s^2$
^1S ^1P ^1D ^1F ^3S ^3P ^3D
$[Kr]\,4d^{10}5s^2\,5p^6\,6s^2$
Ba I
XBL 761-2034 B

Fig. 5

This report was done with support from the United States Energy Research and Development Administration. Any conclusions or opinions expressed in this report represent solely those of the author(s) and not necessarily those of The Regents of the University of California, the Lawrence Berkeley Laboratory or the United States Energy Research and Development Administration.

TECHNICAL INFORMATION DIVISION
LAWRENCE BERKELEY LABORATORY
UNIVERSITY OF CALIFORNIA
BERKELEY, CALIFORNIA 94720